Onset of band structure in ^{70}Ga

R. A. Haring-Kaye and F. Palombi
Department of Physics and Engineering,
Westmont College, Santa Barbara, California, USA

J. Döring
Bundesamt für Strahlenschutz, D-10318 Berlin, Germany

S. L. Tabor, B. Abromeit, R. Lubna,* P.-L. Tai,
Vandana Tripathi, A. Volya, and J. M. VonMoss
Department of Physics, Florida State University, Tallahassee, Florida, USA

D. C. Venegas-Vargas,† C. L. Tan,‡ M. J. Heeschen,§ and K. Q. Le¶
Department of Physics and Astronomy,
Ohio Wesleyan University, Delaware, Ohio, USA

B. L. Harbin**
Department of Physics, Geology, and Engineering Technology,
Northern Kentucky University, Highland Heights, Kentucky, USA

(Dated: March 31, 2022)

Abstract

Excited states in odd-odd ^{70}Ga were studied using the ^{62}Ni(^{14}C,αpn) fusion-evaporation reaction performed at the John D. Fox Superconducting Accelerator Facility at Florida State University with a beam energy of 50 MeV. The depopulating γ decays were measured in coincidence using a Compton-suppressed Ge array consisting of three Clover detectors and seven single-crystal detectors. An investigation of these coincidences resulted in the addition of 16 new transitions in the ^{70}Ga level scheme, including some which belong to the onset of a new positive-parity band structure likely based on the $\pi g_{9/2} \otimes \nu g_{9/2}$ configuration. Spins and parities were assigned based on directional correlation of oriented nuclei ratios and linear polarization measurements. The excitation energies predicted by shell-model calculations using the JUN45 effective interaction compare favorably with the experimental ones for the positive-parity states, but are generally about 400–500 keV too low for the negative-parity states. Total Routhian surface calculations for the lowest positive-parity configuration with signature $\alpha = 0$ predict significant triaxiality ($\gamma \approx -20^\circ$) with competing non-collective excitations developing at a spin ($J = 8$) that corresponds to the onset of the positive-parity band observed experimentally. The calculations for the lowest negative-parity states with $\alpha = 0$ yielded surfaces that were qualitatively similar.

*Present address: Facility for Rare Isotope Beams, Michigan State University, East Lansing, Michigan, USA.

†Present address: Department of Physics and Astronomy, University of Tennessee, Knoxville, Tennessee, USA, and Physics Division, Oak Ridge National Laboratory, Oak Ridge, Tennessee, USA.

‡Present address: Department of Physics and Astronomy, University of Rochester, Rochester, New York, USA.

§Present address: Henway Technologies, Hudson, Ohio, USA.

¶Present address: Department of Mathematics, Temple University, Philadelphia, Pennsylvania, USA.

**Present address: Trane Technologies, Louisville, Kentucky, USA.

I. INTRODUCTION

A hallmark characteristic of odd-odd nuclei in the mass $A \sim 70$ region is a complex low-lying excitation spectrum with high level density, owing to an intrinsic two-quasiparticle (2-qp) configuration, and a regular positive-parity band structure at high spin resulting from the $\pi g_{9/2} \otimes \nu g_{9/2}$ intruder configuration. The odd-odd gallium ($Z = 31$) isotopes appear not to be an exception. For example, studies of ^{66}Ga [1, 2] and ^{68}Ga [3] using heavy-ion reactions revealed both a complicated network of single-particle states below an excitation energy of 2 MeV along with the development of a positive-parity band above a 9^+ state observed near 3 MeV. In both cases, a strong sequence of transitions with spin changes of mostly $\Delta J = 1$ dominated the low-lying decay scheme, while an odd-spin positive-parity band reached the highest observed excitation. Both isotopes also possess relatively low-energy first-excited states, a 1^+ state at 44 keV in ^{66}Ga [4] and a 2^+ state at 175 keV in ^{68}Ga [5], typical of odd-odd nuclei in general.

The evolution of structure with increasing angular momentum is much less clear in the heavier odd-odd Ga isotopes, where relatively little is known about high-spin states due to the difficulty in populating these nuclei using heavy-ion reactions with stable beam and target combinations. In the case of ^{70}Ga, the low-spin regime has been studied extensively using light-particle fusion and transfer reactions (see Ref. [6] for a comprehensive list of these works), with many states described theoretically by the spherical shell model. Two investigations using α-particle beams were able to identify a state as high as 2.88 MeV with a firm 9^+ assignment attributed to the $\pi g_{9/2} \otimes \nu g_{9/2}$ configuration [7, 8]. A more recent work populated ^{70}Ga using the ^{55}Mn(^{18}O, $2pn$) reaction and utilized a modern γ detector array, but could add only one $J = (9)$ state to the level scheme, extending it to 3514 keV [9]. Clear evidence of band structure based on $g_{9/2}$ orbital occupation and the possible associated onset of deformation and/or shape changes has yet to be observed in ^{70}Ga.

Lingering questions also surround the existing ^{70}Ga decay scheme. A rather remarkable facet is the surprisingly large energy of 508 keV for the first-excited state (confirmed by multiple studies, e.g., Refs. [10–12]). By comparison, the neighboring odd-odd isotopes ^{66}Ga, ^{68}Ga, and ^{72}Ga have eleven [4], five [5] and sixteen [13] known levels below 500 keV, respectively. This unusual characteristic of ^{70}Ga has yet to be explained. Additionally, the configuration of the 2^- state at 691 keV remains unclear. Single-particle occupations with

the lowest energy cost, such as the one representing a coupling between the ^{69}Ga ground state (with $J^\pi = \frac{3}{2}^-$ [14] resulting from a $p_{3/2}$ proton hole state) and a $g_{9/2}$ neutron cannot produce a 2^- state, calling the negative-parity assignment into question [12]. A weak differential cross section observed for this state using the (d,p) reaction [15] favored an excited proton configuration (such as $\pi p^2_{3/2} f_{5/2}$) coupled to a $g_{9/2}$ neutron, but conclusive evidence for the negative-parity assignment would be helpful to make a decisive interpretation. Other yrast (or near-yrast) states, such as the ones at 2602 and 2652 keV [8], lack spin and/or parity assignments altogether.

The goal of this work was thus to populate ^{70}Ga at high spin in order to search for a possible $\pi g_{9/2} \otimes \nu g_{9/2}$ band as observed in the lighter odd-odd Ga isotopes, as well as to firmly assign spins and parities for as many states as possible. As a result of this study, the onset of both signature partners of a high-spin positive-parity band was observed, and several spin-parity assignments were made based on directional correlation of oriented nuclei ratios and linear polarization measurements. Interpretations of the excitation spectrum were provided within the context of both shell-model and total Routhian surface calculations.

II. EXPERIMENTAL AND ANALYSIS TECHNIQUES

Excited states in ^{70}Ga were populated by the ^{62}Ni(^{14}C,αpn) fusion-evaporation reaction performed at the John D. Fox Superconducting Accelerator Facility at Florida State University (FSU). The long-lived ^{14}C radioactive beam was produced in a Cs sputter ion source with an enriched Fe_3C sample [16]. Beam ions were accelerated to 50 MeV with an average intensity of about 3×10^{10} particles/s and impinged upon a 25 mg/cm^2 ^{62}Ni target, thick enough to stop all recoiling nuclei and unreacted beam. The αpn channel comprised approximately 3% of the total reaction cross section. The γ rays emitted from the reaction products were detected by an array of ten Compton-suppressed Ge detectors. Three Clover detectors and two single-crystal detectors were placed at 90° relative to the beam axis, and two (three) single-crystal detectors were placed at 35° (145°).

A digital data acquisition system, based on the Digital Gamma Finder Pixie16 system [17], was used to record γ-γ coincidences. Approximately 2.0×10^9 coincidence events were recorded from the detector array under a trigger condition of at least a two-fold multiplicity event between any two individual Ge crystals that also satisfied an anti-coincidence with

their respective bismuth germanate (BGO) Compton suppressor. Wave forms from each Ge crystal and BGO photomultiplier tube were sampled at a rate of 100 MHz. The γ-γ coincidence and Compton-suppression logic as well as pulse heights and event arrival times were determined from the wave forms using digital signal processors and field-programmable gate arrays in each channel of the Pixie16 modules. Offline processing of these data led to the removal of all null events and utilized an effective coincidence resolving time of approximately 1 μs set by the hardware trigger. The filtered data were then sorted into a variety of γ-γ coincidence matrices with a dispersion of 0.6 keV/channel. Both the sorting and analysis of the γ-ray spectra were performed using GNUSCOPE, a spectroscopic analysis software package developed at FSU [18, 19].

The γ-ray coincidences used to study the ^{70}Ga level scheme were investigated mostly with background-subtracted spectra projected from matrices of coincidences among the 90° detectors in order to minimize Doppler shifting. Transition energies E_γ were determined by measuring the line centroids for the decays in as many clean gates as possible in the 90° coincidence spectra and averaging the results. Preliminary energy calibrations were obtained from an ^{152}Eu source, then modified to include a broader energy range based on the known energies of several clean γ-ray lines produced in beam. The γ-ray intensities were first determined at 90° either through clean gates on transitions below the lines of interest or from the total projection of 90° detector coincidences. They were then corrected for angular distribution effects using measured a_2 and a_4 coefficients [8, 12] or theoretical ones determined from the spin change of the transition. These coefficients were utilized to deduce A_0, the angle-independent first-order term in the series of Legendre polynomials that describe the experimental intensities as a function of observation angle. Lastly, the A_0 values were normalized to the one obtained for the 691-keV transition, resulting in a final relative intensity I_γ for each transition. The relative efficiency of the detectors as a function of E_γ was determined from the known intensities of a ^{152}Eu calibration source [20] and a standard logarithmic parameterization for Ge detectors. All measured γ-ray energies and intensities for ^{70}Ga are given in Table I.

Spin changes were measured for as many transitions in ^{70}Ga as possible based on directional correlation of oriented nuclei (DCO) ratios, defined according to:

$$R_{\rm DCO} = \frac{I_\gamma(\text{at } 35^\circ, 145^\circ;\ \text{gated by } \gamma_{\rm G} \text{ at } 90^\circ)}{I_\gamma(\text{at } 90^\circ;\ \text{gated by } \gamma_{\rm G} \text{ at } 35^\circ, 145^\circ)}. \quad (1)$$

In order to increase the statistics of the DCO ratio measurement, the analysis was performed using a matrix constructed to exploit the angular symmetry of the FSU Ge array, in which both 35° and 145° detector events were sorted against only the 90° detector events. Based on the geometry of the array, if the gate γ_G represents a stretched electric quadrupole ($E2$) transition, then the DCO ratios for stretched $E2$ transitions as well as for $\Delta J = 0$ transitions are expected to be approximately unity, while $\Delta J = 1$ transitions yield ratios of about 0.5 if the mixing ratio δ is small [21]. All measured DCO ratios are given in Table I.

Parity assignments were inferred from a γ-ray linear polarization measurement, which used the three Clover detectors as Compton polarimeters [22] placed at an average distance of approximately 19.6 cm from the target. Signals from each of the four individual Ge crystals in each Clover detector were processed whenever at least two fired in coincidence with at least one of the single-crystal detectors in the array. The energies measured by each crystal pair were added and sorted into one of two square coincidence matrices depending on whether they represented a perpendicular or parallel scattering event relative to the beam direction. Events that involved a diagonal pair of Clover crystals were not included in the matrices. Spectra representing either perpendicular or parallel scattering were then obtained from background-subtracted gates projected from these square matrices.

The experimental linear polarizations $P_{\rm exp}$ were determined from the perpendicular ($N_\perp$) and parallel ($N_\parallel$) scattering intensities according to

$$P_{\rm exp} = \frac{1}{Q(E_\gamma)} \frac{a(E_\gamma)N_\perp - N_\parallel}{a(E_\gamma)N_\perp + N_\parallel}. \quad (2)$$

An energy-independent relative normalization of $a(E_\gamma) = 1.00(1)$ was determined from a measurement of $N_\perp$ and $N_\parallel$ for the isotropic ($P_{\rm exp} = 0$) lines of a ^{152}Eu source, consistent with a previous measurement [23] using the same three Clover detectors used in this study. The functional form of the polarization sensitivity $Q(E_\gamma)$ was reproduced from the results of Ref. [22], which determined $Q(E_\gamma)$ for a similar Clover detector. As a test of the method and a check for possible systematic errors, the linear polarizations of known $E1$, $E2$, and mixed $M1/E2$ transitions in ^{70}Ge [24, 25] were deduced from the current measurement and found to be in good agreement with previous results [26]. All measured linear polarizations

for transitions in ^{70}Ga are given in Table I.

Theoretical polarizations $P_{\rm thy}$ were calculated as a function of the multipole mixing ratio δ according to the formalism given in Refs. [27, 28]. Some of the angular distribution coefficients a_2 and a_4 used in the calculations were the ones determined experimentally [8]. If experimental angular distribution coefficients were unavailable, or if their uncertainties were too large to deduce meaningful interpretations from the resulting $P_{\rm thy}$ values, theoretical coefficients were determined as a function of δ, based on the spins involved in the transition, using the formalism and sign conventions of Rose and Brink [29]. The resulting array of a_2 and a_4 coefficients could then be used to infer $P_{\rm thy}$ for any desired value of δ, although in general stretched ($\delta = 0$) transitions were assumed. These two methods of deducing $P_{\rm thy}$ converge to predict the same polarization at the value of δ that reproduces the experimental a_2 and a_4 values.

III. RESULTS

The level scheme of ^{70}Ga deduced from the present work is shown in Fig. 1. Most of the yrast states and associated transitions observed in the last published high-spin study [8] were confirmed. Overall, 16 new transitions were assigned to ^{70}Ga in this work. Most of these transitions can be identified in a spectrum gated on the low-lying 188-keV transition, as shown in Fig. 2. This has led to the discovery of 6 new states, reaching a spin and excitation energy as high as an (11^+) state at 4428 keV. The supporting evidence for the level scheme enhancements is discussed in the subsections that follow.

A. Negative-parity states

The strong sequence of transitions between yrast negative-parity states below 1400 keV, which dominates the low-spin structure of the ^{70}Ga level scheme, has been confirmed. In particular, the spin and parity assignments of the yrast levels have been verified through DCO ratio and linear polarization measurements (see Table I). A 2^- assignment for the 691-keV state thus appears firm, the implications of which will be discussed in Sec. IV.

Two other low-lying states observed in Ref. [8], a $J = 5$ level at 1180 keV and another with $J^\pi = (6)^-$ at 1540 keV (measured at 1538 keV in this work), now have firm spin-parity

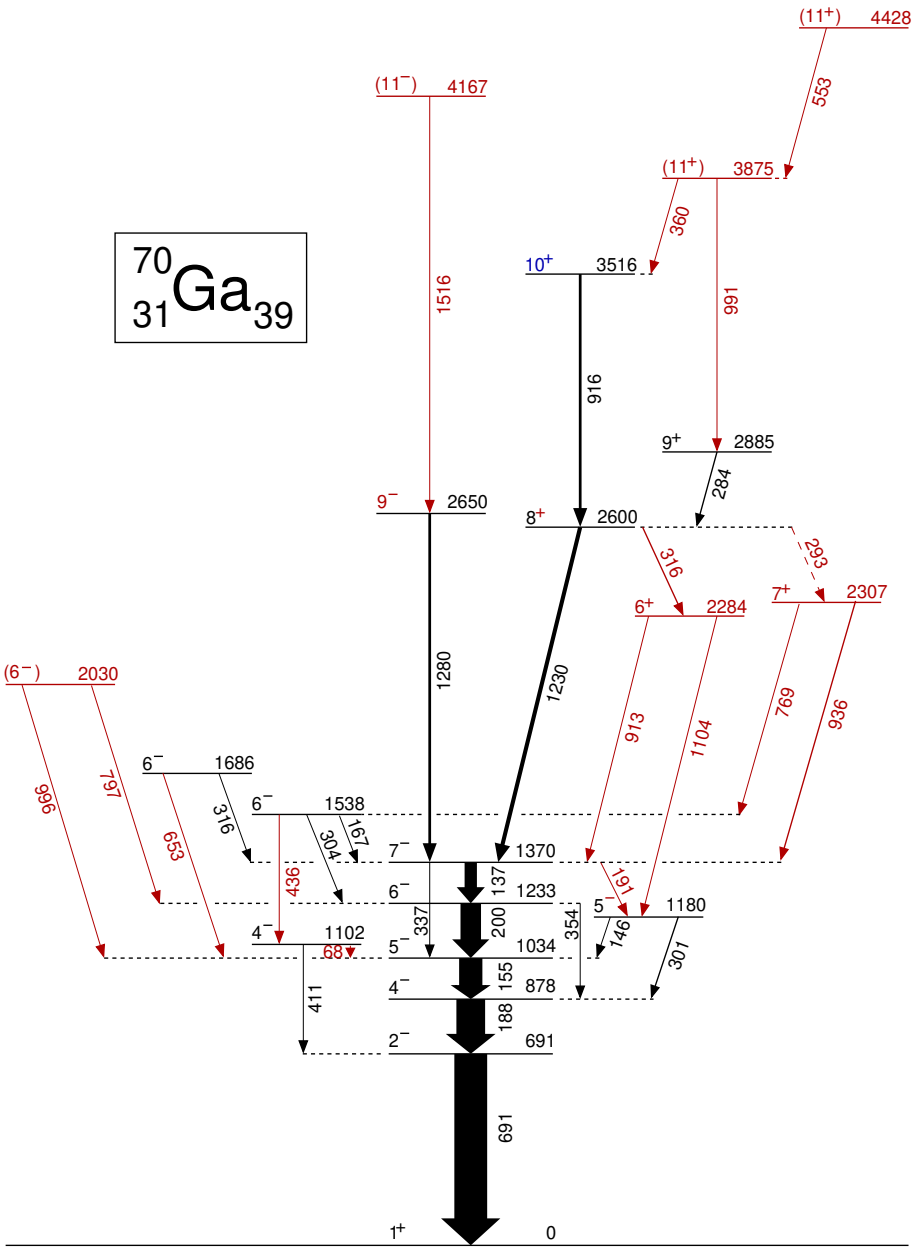

FIG. 1: Partial level scheme of ^{70}Ga deduced from the present work. Transitions, states, and spin-parity assignments shown in red are new to this study, while those indicated in black have been verified from previous investigations. Spin and/or parity assignments modified from previous works are shown in blue.

assignments. The 1180-keV state has been assigned $J^\pi = 5^-$ based on the observation of a new 191-keV transition between the 7^- state at 1370 keV and this one, which is consistent with $\Delta J = 2$ and thus almost certainly $E2$ character based on its measured DCO ratio of

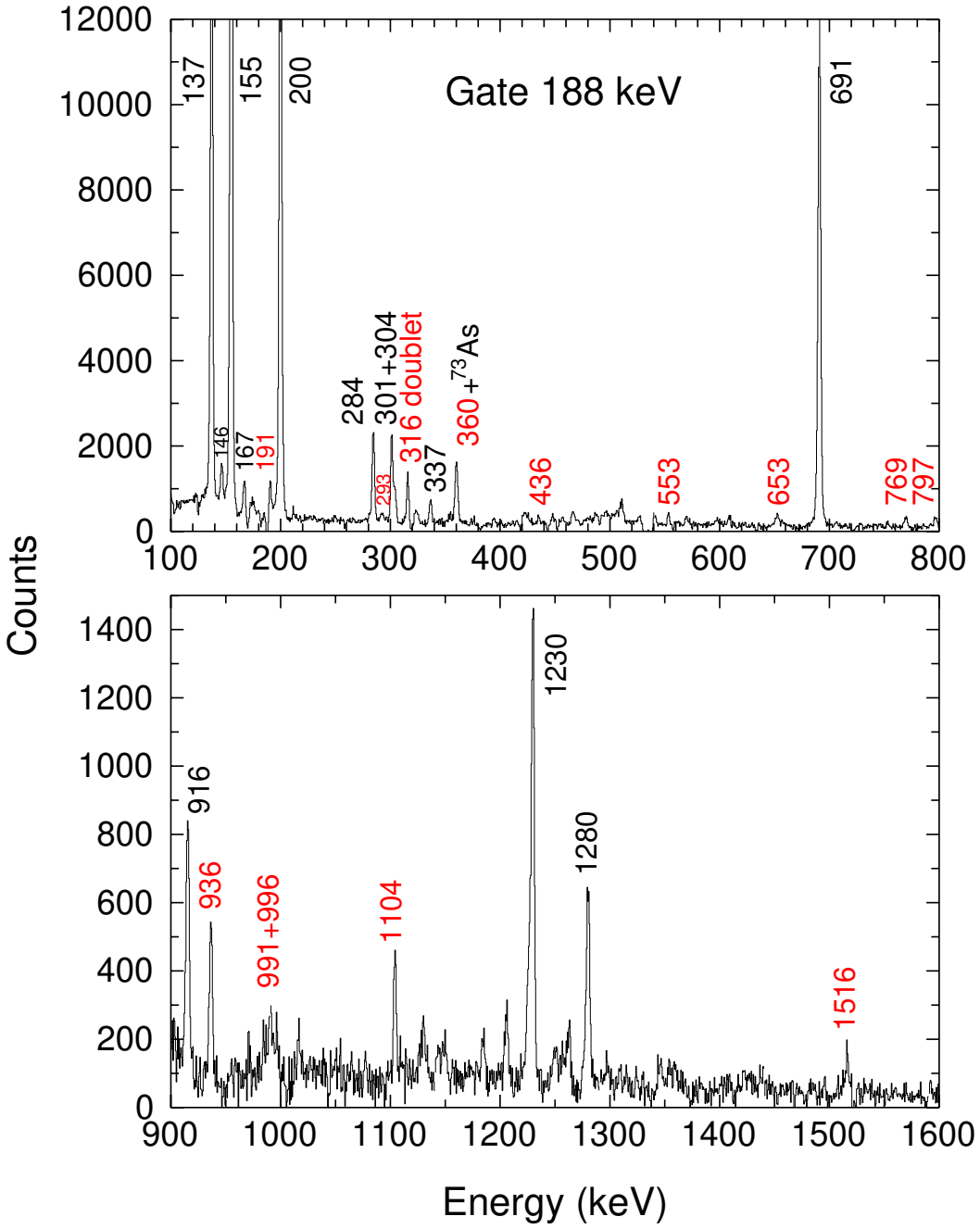

FIG. 2: A portion of the 90° background-subtracted coincidence spectrum obtained by gating on 188-keV γ rays. New transitions in the ^{70}Ga level scheme, as determined in this work, have their energies labeled in red.

0.9(3). Meanwhile, the proposed 6^- assignment for the 1540-keV state [8] (1538 keV in this work) is supported by both the measured DCO ratios of the 167- and 304-keV transitions and the non-yrast nature of this state. Further evidence for this spin-parity assignment comes

from the observation of a new 436-keV transition to a known [6] 1102-keV level, which has been assigned $J^\pi = 4^-$ based on a measured DCO ratio of 1.5(6) for its 411-keV decay using the 691-keV $E1$ gate, a result consistent with those of other $E2$ transitions measured from this gate. This assignment agrees with the previous suggestion of $J^\pi = (3,4)^-$ [6]. Moreover, the 6^- state at 1689 keV [8] (1686 keV in this study) was confirmed through the observation of a 653-keV transition between this state and the 5^- state at 1034 keV. A new level at 2030 keV, which could be another non-yrast 6^- state, was identified from the coincidence relations between 797- and 996-keV γ rays and known low-lying transitions in ^{70}Ga. Interestingly, the 653 and 797 keV lines were identified previously (see Fig. 4 in Ref. [8]) but not placed in the ^{70}Ga decay scheme.

At higher excitation, a 2652-keV state (2650 keV in this work), first observed from its 1280-keV decay to the 7^- state at 1370 keV [8], was confirmed and assigned a spin-parity for the first time of $J^\pi = 9^-$ based on both a DCO ratio and linear polarization measurement for the 1280-keV transition consistent with $E2$ radiation (see Table I). A weak 1516-keV line was found to be in mutual coincidence with 1280-keV γ rays as well as the strong sequence of decays below the 1370-keV state, establishing a new level at 4167 keV. The measured DCO ratio of the 1516-keV transition favors, but does not uniquely establish, quadrupole (and very likely $E2$) character for this decay, leading to a tentative (11^-) assignment for this new state.

B. Positive-parity states

Four new positive-parity states have been identified in this work, while two other states have been firmly assigned positive parity for the first time. Of these, the $J = 8$ state at 2602 keV [8] (2600 keV in this work) appears to be the head of a new positive-parity band structure in ^{70}Ga. Previously, this state was speculated to be a member of the $(\pi g_{9/2} \otimes \nu g_{9/2})$ multiplet [8]. However, no conclusive parity determination was made, and even the spin assignment was considered somewhat tentative due to the uncertainties involved with the angular distribution measurement of the 1230-keV decay depopulating this level [8]. In this work, the dipole nature of this transition was conclusive based on a measured DCO ratio of 0.48(13). Although the measured polarization of $P_{\rm exp} = +0.3(3)$ for this line agrees best with the predicted result of $P_{\rm thy} = +0.3(6)$ based on the corresponding a_2, a_4, and

δ values determined experimentally [8] and assuming a parity-changing $E1$ transition, the large relative uncertainty in $P_{\rm thy}$ calculated this way casts doubt on the interpretation of the measured polarization. However, when comparing the experimental polarization of the 1230-keV transition to purely theoretical ones as a function of δ, as shown in Fig. 3, the $P_{\rm exp}$ value only agrees with theoretical values corresponding to $E1/M2$ radiation within the range of δ values allowed by the previous measurement ($\delta = 0.0(2)$, corresponding to $|\arctan(\delta)| < 11^\circ$) [8]. In particular, the agreement is excellent at $\delta = 0$, which is most likely for $E1$ decay. Thus the 1230-keV has been confidently identified as an $E1$ transition, leading to a firm 8^+ assignment for the 2600 keV state.

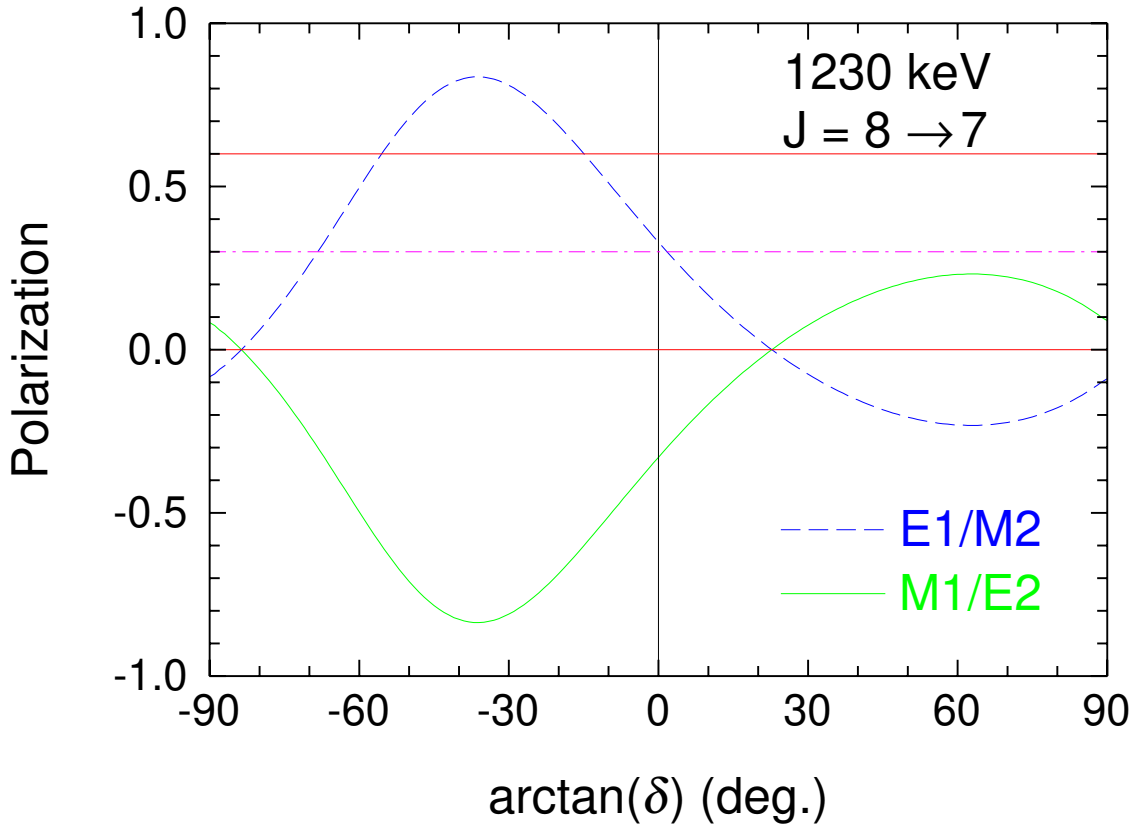

FIG. 3: The measured (dot-dashed line) and theoretically expected (solid and dashed curves) polarizations as a function of the multipole mixing ratio δ for the 1230-keV transition. The solid horizontal lines indicate the experimental uncertainty limits.

Progressing to higher spin, a 3516-keV state was discovered previously from a 916-keV decay to the 2600 keV state with a suggested spin of $J = (9)$ [9]. However, our measured DCO ratio of 0.9(2) for the 916-keV line strongly suggests a stretched $E2$ transition, which

is further supported by its linear polarization of 0.6(6). This new evidence points to a 10^+ assignment for the 3516-keV state and the onset of a signature $\alpha = 0$ sequence with positive parity.

We have confirmed the 9^+ assignment attributed to the 2887-keV state [7, 8] (2885 keV in this study) through a measurement of the DCO ratio [0.51(7)] and linear polarization [−0.5(3)] for its 284-keV decay. Above this state, the start of an $\alpha = 1$ partner band appears to be established by the observation of a 991-keV transition between a new (11^+) state at 3875 keV and the 9^+ state, although the spin and parity of this new state remains tentative due to the relatively weak counting statistics associated with the 991-keV line in the spectra used for the DCO ratio and linear polarization analyses. A clean 990-keV peak was also observed in a sum coincidence gate on the 188- and 691-keV transitions using the ^{68}Zn(α, pn) reaction but not placed in the ^{70}Ga level scheme [8]. Further confirmation for the 3875-keV state comes from the observation of a 360-keV transition from this state to the 10^+ state. A second (11^+) state was found at 4428 keV based on its decay to the lower (11^+) state. The tentative (11_2^+) assignment stemmed from an assumption of $\Delta J = 0$ character for the 553-keV transition based on its DCO ratio of 1.0(4). This possibility seemed more likely than $\Delta J = 2$ nature for the 553-keV decay given that a similar non-yrast $J = (11)$ state was observed in ^{68}Ga [3] with an excitation energy and decay pattern that closely resembles this one.

Additional positive-parity states were observed at 2284 and 2307 keV with $J^\pi = 6^+$ and 7^+, respectively. Previously, a single 316-keV transition was placed between a 6^- state at 1689 keV and the 7^- state at 1372 keV [8], which we could confirm (see Sec. III A). However, our observed coincidence relationships favor a second, and stronger, 316-keV transition between the 8^+ state at 2600 keV and a new 6^+ level at 2284 keV. The spin and parity of this new level were inferred from a measured DCO ratio of 0.85(18) for the 316-keV doublet (dominated by the stronger transition), favoring $E2$ decay, and 0.5(2) for the 1104-keV transition, pointing to dipole radiation. The new state at 2307 keV was established by its measured decays of 769 and 936 keV as well as a weak 293-keV transition from the 8^+ state at 2600 keV to this one. The firm 7^+ assignment is based on both the measured DCO ratio [1.1(2)] and linear polarization [−0.7(8)] of the 936-keV transition, which together favor $E1$ radiation with $\Delta J = 0$. Both the 936- and 1104-keV lines were also seen previously in clear coincidence with 188- and 691-keV γ rays but not placed in the level scheme [8].

A low-lying, even-spin sequence of positive-parity levels (not shown in Fig. 1) including the 2^+ first-excited state at 508 keV, a 4^+ state at 902 keV decaying by a 393-keV γ ray, and a (6^+) state at 1087 keV decaying by a 185-keV γ ray was reported in Ref. [8] without any feeding from the high-spin yrast sequence. The lowest two states had already been established [30] but the 1087-keV state was not verified by a more recent study [6]. We can confirm the coincidence of the 393-keV transition with the low-lying 508-keV transition, verifying the two lowest levels of this sequence. No linking transitions to levels shown in Fig. 1 were found.

IV. DISCUSSION

Previous work interpreted the observed ^{70}Ga level spectrum within the context of the parabolic rule derived from the cluster-vibration model [6] and, more recently, large-scale shell-model calculations using the JUN45 effective interaction [9]. Since additional spin-parity assignments are now available and the level scheme has been extended to higher spin, we performed similar shell-model calculations to test the performance of this interaction at an excitation energy where collective behavior becomes increasingly important in ^{66}Ga [1, 2]. Total Routhian surface (TRS) calculations following the cranked Woods-Saxon approach [31] were performed in order to see if the onset of the observed positive-parity band corresponds to a predicted increase in deformation and/or shape changes at the associated spin. This new positive-parity structure, which likely corresponds to the $\pi g_{9/2} \otimes \nu g_{9/2}$ configuration, resembles other high-spin positive-parity bands in neighboring odd-odd nuclei. Systematic trends in other yrast (or near-yrast) states were also explored between ^{70}Ga and its neighbors. The results of these various interpretive calculations are described in the subsections that follow.

A. Shell-model calculations

In order to help understand the microscopic structure of ^{70}Ga, shell-model (SM) calculations were performed using the COSMO code [32] incorporating the JUN45 effective interaction [33], which uses a ^{56}Ni core and allows unrestricted occupation of the $1p_{3/2}$, $0f_{5/2}$, $1p_{1/2}$, and $0g_{9/2}$ orbitals for both protons and neutrons. A rich excitation spectrum was produced,

consisting of over 200 states spanning to a maximum energy of 6.046 MeV (a non-yrast 11^- state). Of these, 6 excited states are predicted below an excitation energy of 510 keV, in contrast to the single level observed experimentally. In fact, the calculations predict a first-excited 2_1^+ state at 36 keV, underscoring the difficulty in replicating the experimental energy ($E_1 = 508$ keV) and pointing to a remaining challenge for future calculations that might incorporate a larger number of active nucleons.

A comparison between the yrast states in ^{70}Ga observed from high-spin population in this work (see Fig. 1) and the corresponding states predicted by the SM calculations is illustrated in Fig. 4. The results for the positive-parity states are reasonable, but not as good as, for example, those of the USD family of interactions for lighter nuclei [34]. The results for the negative-parity states are about 400 to 500 keV too low, but would achieve about the same level of agreement with experiment if shifted up by this amount.

The wave functions derived from the SM calculations also yield orbital occupancies, which can shed light on the configurations responsible for the states observed experimentally. In particular, the lowest 2^- state is predicted to consist (on average) of approximately two protons (1.67) in the $p_{3/2}$ state, one proton (1.02) in the $f_{5/2}$ state, and two neutrons (2.10) in the $g_{9/2}$ state, lending support to the excited configuration responsible for this state proposed previously [15]. Virtually no protons (0.13) are predicted to occupy the $g_{9/2}$ orbital for this state. In contrast, the proton $g_{9/2}$ orbital occupation becomes closer to one (0.66) for the lowest 8^+ and 9^+ states, corresponding to the onset of the positive-parity band structure observed in this work. By comparison, the neutron $g_{9/2}$ occupation increases to 2.69 particles in the 8_1^+ configuration, but falls to 2.11 particles for the 9_1^+ state. This overall increased participation of protons and neutrons in the $g_{9/2}$ orbital might be expected to trigger increased collectivity and/or shape changes, as will be explored in Sec. IV C.

To provide some calibration of the JUN45 interaction in this mass region, a comparison between the lowest negative-parity states observed experimentally and the corresponding ones predicted by this interaction for ^{69}Ga and ^{71}Ga is shown in Fig. 5. The agreement between the experimental and theoretical energies is generally favorable, with root-mean-square differences of 116 and 142 keV for ^{69}Ga and ^{71}Ga, respectively. Not enough positive-parity states are known experimentally to justify a figure. However, the $9/2^+$ states are known in both nuclei and are predicted 534 and 984 keV too high, respectively. Although the differences are in the opposite direction compared to ^{70}Ga, it is clear that JUN45 cannot

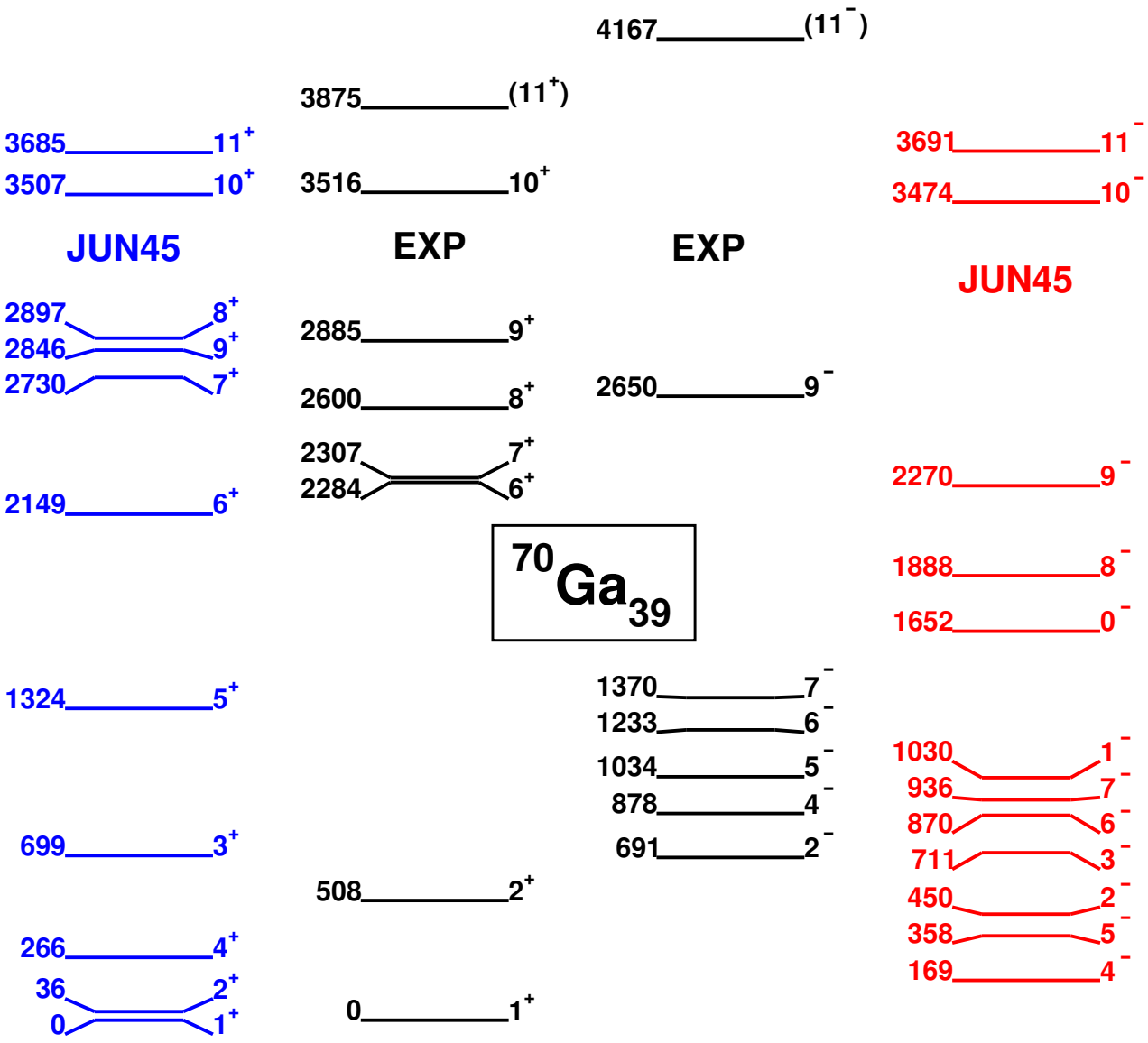

FIG. 4: A comparison of the experimental yrast level energies in ^{70}Ga observed in this work with the corresponding theoretical ones predicted by shell-model (SM) calculations using the JUN45 interaction.

predict the effective $N = 40$ gap very well in these nuclei. Also, not allowing excitations out of the $0f_{7/2}$ orbital may not be a good approximation for the Ga isotopes with only three protons above the shell closure.

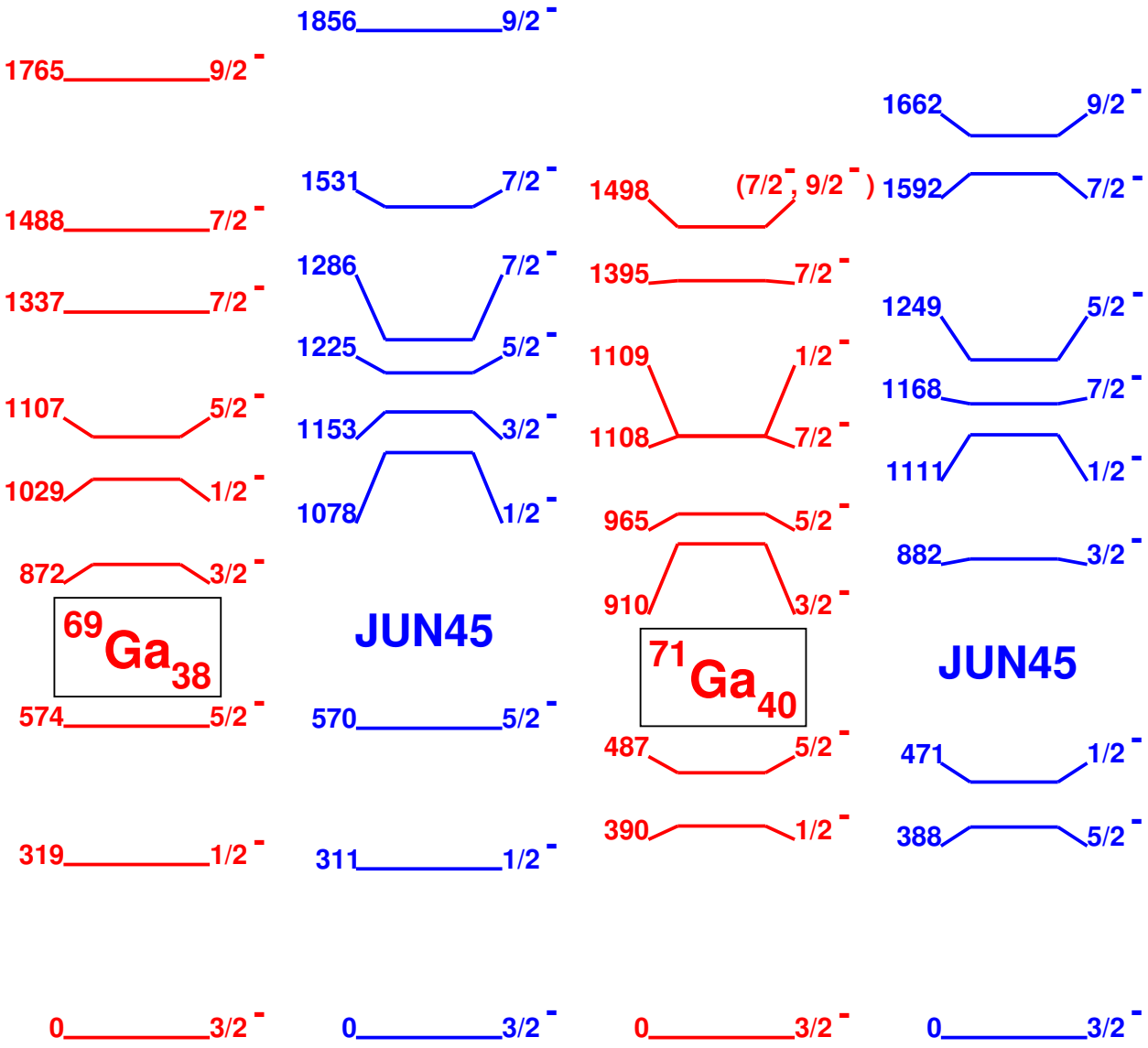

FIG. 5: A comparison of the lowest experimental negative-parity level energies in ^{69}Ga [14] and ^{71}Ga [35] with the corresponding theoretical ones predicted by shell-model (SM) calculations using the JUN45 interaction.

B. Systematic comparisons

A comparison of the yrast and near-yrast states of ^{70}Ga ($N = 39$) with other odd-odd Ga isotopes is shown in Fig. 6. Despite the lack of several firm spins and parities for $A \leq 66$, a strong family resemblance can be seen among these isotopes even with the suggested assignments. In general, a trend of decreasing excitation energy with increasing neutron number can be seen. One should also keep in mind some variability in which states can be

seen experimentally from γ cascades depending on the exact ordering of the levels. From a microscopic point of view, both the odd proton ($Z = 31$) and neutron would be expected to lie primarily in negative-parity fp orbitals in the lowest energy states, giving an overall positive parity, as is seen in all of these isotopes. The highest spin possible purely within the fp shell and without breaking and recoupling any pairs is 5^+ from the $\pi f_{5/2} \otimes \nu f_{5/2}$ configuration. No states with a confident assignment of 6^+ have been reported near 5^+ ones in these nuclei, pointing to the additional energy cost needed to break a nucleon pair and generate a 6^+ state.

Promotion of the uncoupled neutron to the positive-parity $0g_{9/2}$ intruder orbital would provide the highest spin increment at the least energy cost, a cost that would increase with decreasing neutron number. Such states would have negative parity. Evidence for this trend is seen in the odd-odd Ga isotopes shown in Fig. 6, at least down to ^{64}Ga. The increasing excitation energies of the negative-parity states allows more positive-parity states to be yrast and more visible experimentally. Above the lowest 7^- state there is a gap of about 1 MeV to the state of next higher spin. We note that $J^\pi = 7^-$ corresponds to the highest spin available from the $\pi f_{5/2} \otimes \nu g_{9/2}$ configuration without breaking and recoupling pairs of any other nucleons. Higher spins of either parity would require breaking pairs and either recoupling to higher spin (up to $2\hbar$ [$4\hbar$] for a $p_{3/2}$ [$f_{5/2}$] pair) or promoting to the $g_{9/2}$ orbital.

In order to explore the onset of positive-parity band structure in these nuclei, the normalized energy differences between states differing by $\Delta J = 1$ as a function of the initial-state spin J_i for the lowest positive-parity states that form a band structure in the ^{66}Ga and ^{70}Ga isotopes are shown in Fig. 7 along with the corresponding pattern for ^{72}As [39, 40]. (The ^{68}Ga isotope was not included in the comparison due to a lack of firm spin-parity assignments. Also, the $J = 7$ state at 1179 keV in ^{72}As was assumed to have positive parity.) Such energy differences are indicative of the degree of signature splitting between the favored and unfavored decay sequences of a given intrinsic configuration and tend to be sensitive to underlying structural properties. As illustrated in the figure, the alternating patterns are qualitatively similar to each other for $J > 8$, indicative of a common $\pi g_{9/2} \otimes \nu g_{9/2}$ configuration. In this mass region, such patterns are commonly observed in the lowest positive-parity bands of odd-odd nuclei and have been explained within the context of a two-qp-plus-rotor model [41] in terms of how two unlike $g_{9/2}$ nucleons couple to the core rotation. Below $J = 9$ (the maximum spin obtained from two unlike $g_{9/2}$ nucleons), both qp-spin realignment and

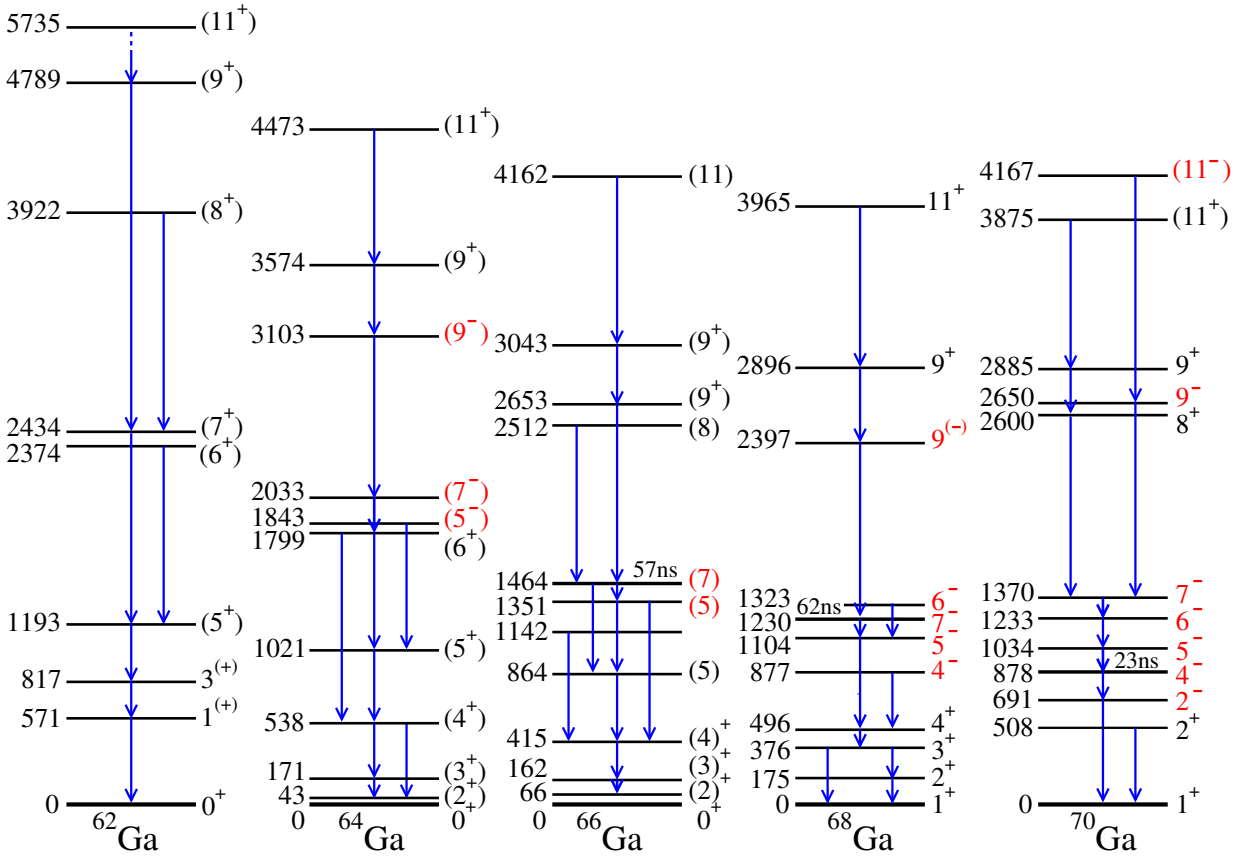

FIG. 6: Partial level schemes of ^{62}Ga [36], ^{64}Ga [37], ^{66}Ga [4], ^{68}Ga [5], and ^{70}Ga showing a comparison of the yrast and near-yrast states observed experimentally, including selected half-life measurements. States with negative (positive) parity are shown with their spin-parity labels in red (black). The half-life of the 4^- isomeric state in ^{70}Ga has been taken from Ref. [30]. The low-lying 1^+ state at 44 keV in ^{66}Ga has been omitted for clarity. Furthermore, individual studies of ^{66}Ga provide different spin-parity assignments for a number of low-lying levels, e.g., for the $I = (7)$ level at 1464 keV. Negative parity is given in Ref. [38] based on lifetime and g-factor measurements, whereas a 7^+ assignment is deduced in Refs. [1, 2].

core rotation contribute to the angular momentum, leading to even-spin states lying relatively lower in energy than the odd-spin ones, while for $J > 9$ collective motion dominates and consequently the odd-spin states are favored once the two qp spins are fully aligned with the core rotation. The model further suggests that the spin at which the resulting phase reversal occurs depends on the residual proton-neutron interaction.

Good qualitative agreement was also observed for $J > 8$ between the signature-splitting pattern predicted by SM calculations and the experimental one in ^{70}Ga, with the best quan-

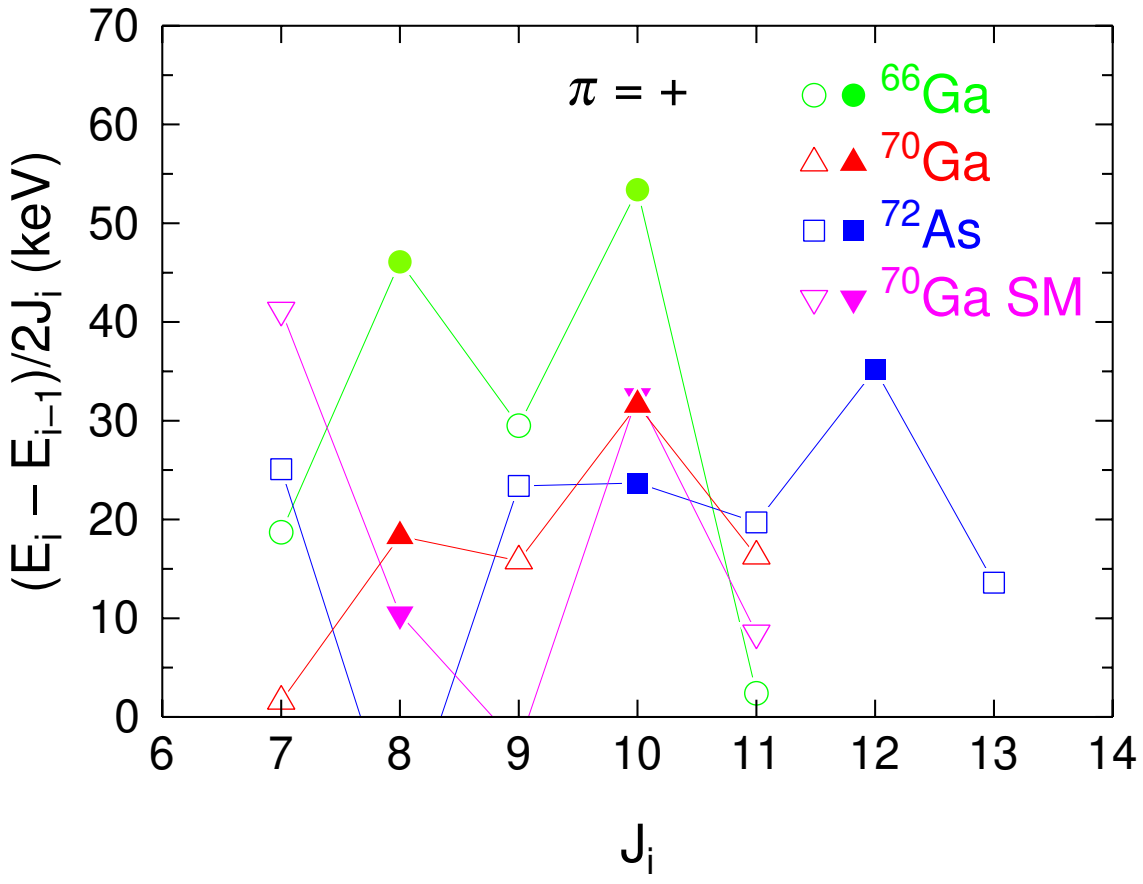

FIG. 7: Normalized energy differences between adjacent states as a function of the spin J_i of the initial state for the yrast positive-parity decay sequences in ^{66}Ga [1], ^{70}Ga, and ^{72}As [39, 40]. Theoretical values predicted by shell-model (SM) calculations for the yrast positive-parity sequence in ^{70}Ga are also included. Filled (open) symbols are used for states with even (odd) J_i.

titative agreement occurring at $J_i = 10$ and 11. Correspondingly, the predicted excitation energies for the 9^+ and 10^+ states are in especially good agreement with the observed ones (see Fig. 4). On the other hand, the SM calculations do not predict the energy of the 11^+_1 level nearly as well and the 8^+ state is predicted to lie higher in energy than the 9^+ level, contrary to observation. Probing deeper, the average proton occupation of the $g_{9/2}$ orbital drops from 0.66 in the 8^+ and 9^+ states to 0.13 (0.10) in the 10^+ (11^+_1) state while the neutron occupation of this orbital fluctuates between 2.1 and 2.4. The decreasing average $g_{9/2}$ proton occupations with spin do not support an aligned $\pi g_{9/2} \otimes \nu g_{9/2}$ configuration and could instead point to non-collective excitations. This is in sharp contrast to similar SM calculations performed for ^{66}Ga, which indicated proton (neutron) $g_{9/2}$ orbital occupancies of

0.41 (1.82) for the 10^+ state and 0.94 (1.31) for the 11_1^+ state [1], likely indicating enhanced collectivity with spin.

C. TRS calculations

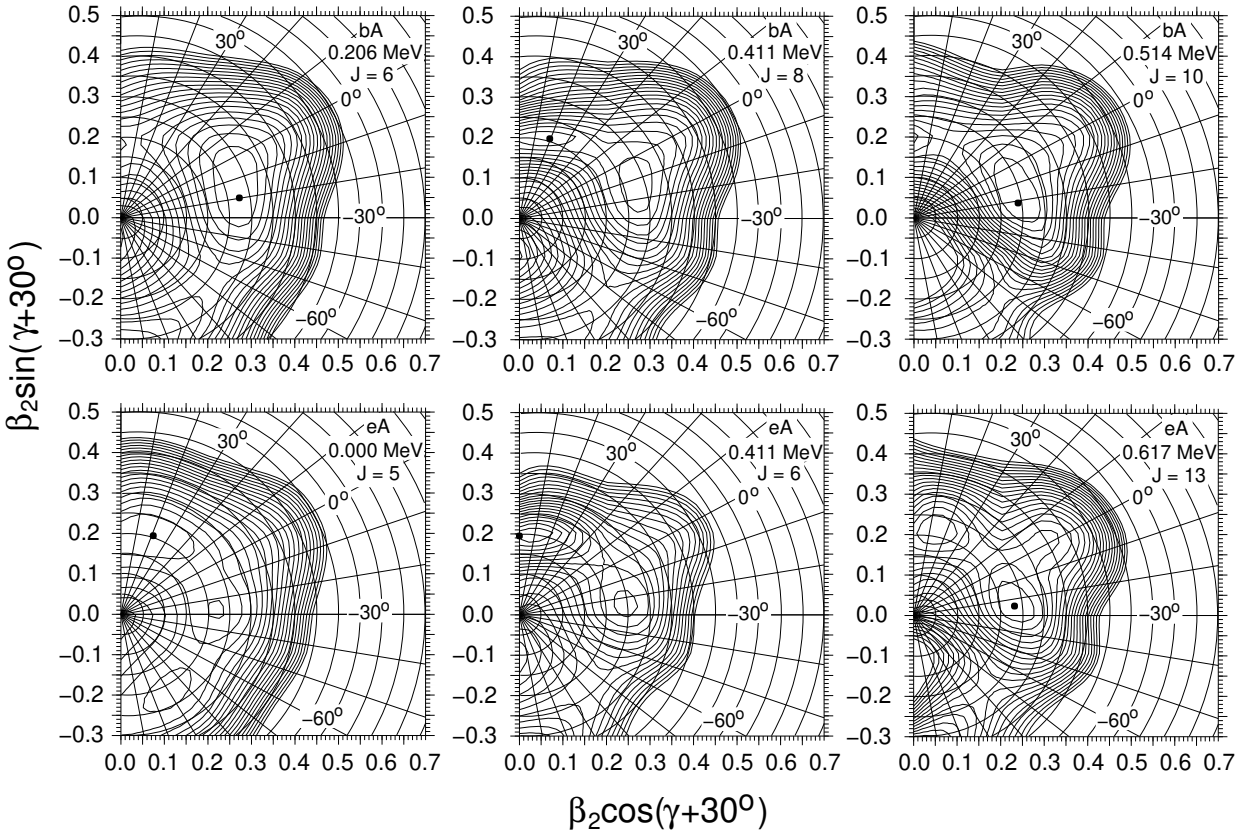

FIG. 8: Sample total Routhian surfaces in the (β_2, γ) plane for the lowest positive- (top) and negative-parity (bottom) configurations in ^{70}Ga at the rotational energies (and their corresponding approximate spin J) indicated in each plot. The bA (eA) configuration corresponds to states with positive (negative) parity and signature $\alpha = 0$. The spacing between contour lines is 200 keV.

The TRS calculations performed in this work explored the evolution of shape and deformation with spin for configurations representing yrast positive- and negative-parity states in ^{70}Ga. The calculations generate TRS contour plots as a function of the quadrupole deformation (β_2) and shape (γ) parameters in a polar-coordinate plane at discrete rotational frequencies, using a deformed Woods-Saxon potential and a short-range monopole pairing force [31]. At each grid point, the Routhian was minimized with respect to the hexadecapole

deformation β_4.

Figure 8 shows six representative TRS plots at different rotational frequencies (and their corresponding approximate spin J) for intrinsic configurations corresponding to the lowest positive- (top) and negative-parity (bottom) states with signature $\alpha = 0$ available in the calculations. The qp-labeling scheme of Ref. [42] was used, where lower (upper) case letters are used for the proton (neutron) configuration. Thus, the bA (eA) case stands for the lowest two-qp configuration yielding overall positive (negative) parity and $\alpha = 0$. Similar results were obtained for the lowest configurations that lead to $\alpha = 1$ states.

Below the onset of the new band structure, the positive-parity states show a rather diffuse collective minimum with modest deformation ($\beta_2 = 0.28$) and significant triaxiality ($\gamma = -20°$). At the observed band head ($J = 8$), the same collective minimum persists but competes with a non-collective one ($\beta_2 = 0.21$, $\gamma = 40°$) which represents the absolute minimum in the surface. When the spin reaches the highest observed experimentally for this signature ($J = 10$), the near-triaxial collective minimum once again becomes favored. The surfaces at higher spins resemble the one shown for $J = 8$, with similar non-collective minima lying lowest in energy.

Representative results for negative-parity states using the eA configuration are shown in the bottom row of Fig. 8. This configuration could represent some of the low-lying yrast states described by the $\pi p_{3/2} \otimes \nu g_{9/2}$ configuration [8]. The surfaces are rather similar to the ones indicated for the bA configuration over a similar spin range. At the lowest frequency, a highly γ-soft surface is produced, with a near-triaxial collective minimum competing with a non-collective one. This picture persists with increasing frequency, although the minima become somewhat more pronounced. When the rotational energy reaches 0.617 MeV ($J = 13$), the (mostly) triaxial minimum becomes lowest but a non-collective one still competes favorably.

V. SUMMARY

The level scheme of ^{70}Ga was enhanced to include 16 new transitions, some of which form the onset of a positive-parity band structure observed for the first time. The low-spin yrast decay sequence, as populated from high-spin decay, has mostly been verified. Several spin and parity assignments were made from directional correlation of oriented nuclei ratios and

linear polarization measurements.

Shell-model calculations utilizing the JUN45 effective interaction generally reproduce the experimental positive-parity excitation spectrum better than the negative-parity one, pointing to an inability of this interaction in predicting the effective $N = 40$ shell gap for the Ga isotopes. JUN45 also fails to account for the unusually high first excited-state energy (508 keV) in ^{70}Ga. Although the calculations replicate the qualitative features of the observed signature splitting between the even- and odd-spin members of the new positive-parity band above spin $J = 9$, the predicted average $g_{9/2}$ orbital occupations are inconsistent with an aligned $\pi g_{9/2} \otimes \nu g_{9/2}$ configuration for states with $J > 9$ that is typical of other yrast positive-parity bands in this mass region. The small $g_{9/2}$ occupancies could point to non-collective behavior. Overall, the increasing body of experimental data to which this paper contributes and the limitations of JUN45 also demonstrated in this work justify and provide a basis for additional theoretical work in this mass region.

Total Routhian surface calculations indicate mostly γ-soft collective shapes with significant triaxiality which compete with non-collective excitations. For the lowest positive-parity states, non-collective minima first become energetically favored at the spin at which the new positive-parity band emerges ($J = 8$), then continue to have similar energies as the collective near-triaxial minima as the spin increases. The evolution of shape with spin is qualitatively similar for the lowest negative-parity states.

Acknowledgments

This work was supported by the U. S. National Science Foundation through Grant No. PHY-14-01574 (FSU) and Research Experience for Undergraduates (REU) Program Grant No. 1658998 (OWU); the U. S. Department of Energy Office of Science, Office of Nuclear Physics under Grant No. DE-SC0009883; and the Ohio Wesleyan University Summer Science Research Program. We are grateful to the staff of the FSU John D. Fox Superconducting Accelerator Facility for their support throughout the experiment, and to W. Nazarewicz for providing the results of his cranked Woods-Saxon calculations. Collabora-

tion with N. H. Medina at the Universidade de São Paulo was a fruitful part of this study.

---

[1] S. S. Bhattacharjee, R. P. Singh, S. Muralithar, Indu Bala, R. Garg, S. Rajbanshi, D. Singh, A. Dhal, M. Kumar Raju, S. Saha, J. Sethi, and R. Palit, Phys. Rev. C **95**, 054330 (2017).

[2] U. S. Ghosh, S. Rai, B. Mukherjee, A. Biswas, A. K. Mondal, K. Mandal, A. Chakraborty, S. Chakraborty, G. Mukherjee, A. Sharma, I. Bala, S. Muralithar, and R. P. Singh, Phys. Rev. C **102**, 024328 (2020).

[3] A. K. Singh, G. Gangopadhyay, D. Banerjee, R. Bhattacharya, R. K. Bhowmik, S. Muralithar, R. P. Singh, A. Goswami, S. Bhattacharya, B. Dasmahapatra, and S. Sen, Eur. Phys. J. A **9**, 197 (2000).

[4] E. Browne and J. K. Tuli, Nucl. Data Sheets **111**, 1093 (2010).

[5] E. A. McCutchan, Nucl. Data Sheets **113**, 1735 (2012).

[6] T. Fényes, J. Gulyás, T. Kibédi, A. Krasznahorkay, J. Timár, S. Brant, and V. Paar, Nucl. Phys. A **419**, 557 (1984).

[7] C. C. Lu, M. S. Zisman, and B. G. Harvey, Phys. Rev. **186**, 1086 (1969).

[8] C. Morand, M. Agard, J. F. Bruandet, A. Giorni, J. P. Longequeue, and Tsan Ung Chan, J. Phys. (Paris) **38**, 105 (1977).

[9] P. R. P. Allegro, Ph. D. thesis, Universidade de São Paulo, 2013.

[10] S. E. Arnell, H. Linusson, and Z. Sawa, Nucl. Phys. A **166**, 241 (1971).

[11] J. Vervier and H. H. Bolotin, Phys. Rev. C **3**, 1570 (1971).

[12] M. R. Najam, L. E. Carlson, W. F. Davidson, and W. M. Zuk, Nucl. Phys. A **211**, 77 (1973).

[13] D. Abriola and A. A. Sonzogni, Nucl. Data Sheets **111**, 1 (2010).

[14] C. D. Nesaraja, Nucl. Data Sheets **115**, 1 (2014).

[15] D. A. Dohan and R. G. Summers-Gill, Nucl. Phys. A **241**, 61 (1975).

[16] R. Maier, G. Korschinek, P. Spolaore, W. Kutschera, H. J. Maier, and W. Goldstein, Nucl. Instrum. Methods **155**, 55 (1978).

[17] XIA LLC, `http://www.xia.com/DGF_Pixie16.html/`

[18] J. Pavan, Ph. D. thesis, Florida State University, 2003.

[19] `[http://fsunuc.physics.fsu.edu/~caussyn/]`.

[20] Table of Isotopes, ed. R. B. Firestone and V. S. Shirley, Eighth Edition (Wiley-Interscience,

New York, 1996).

[21] E. F. Moore, P. D. Cottle, C. J. Gross, D. M. Headly, U. J. Hüttmeier, S. L. Tabor, and W. Nazarewicz, Phys. Rev. C **38**, 696 (1988).

[22] P. M. Jones, L. Wei, F. A. Beck, P. A. Butler, T. Byrski, G. Duchêne, G. de France, F. Hannachi, G. D. Jones, and B. Kharraja, Nucl. Instrum. Methods Phys. Res. A **362**, 556 (1995).

[23] R. A. Kaye, C. S. Myers, J. Döring, S. L. Tabor, S. M. Gerbick, T. D. Baldwin, D. B. Campbell, C. Chandler, M. W. Cooper, M. A. Hallstrom, C. R. Hoffman, J. Pavan, L. A. Riley, and M. Wiedeking, Phys. Rev. C **78**, 037303 (2008).

[24] C. Morand, M. Agard, J. F. Bruandet, A. Giorni, J. P. Longequeue, and Tsan Ung Chan, Phys. Rev. C **13**, 2182 (1976).

[25] R. L. Robinson, H. J. Kim, R. O. Sayer, J. C. Wells Jr., R. M. Ronningen, and J. H. Hamilton, Phys. Rev. C **16**, 2268 (1977).

[26] L. Cleemann, U. Eberth, J. Eberth, W. Neumann, and V. Zobel, Phys. Rev. C **18**, 1049 (1978).

[27] Takayoshi Aoki, Kohei Furuno, Yoshihiro Tagishi, Susumu Ohya, and Jian-Zhi Ruan, At. Data Nucl. Data Tables **23**, 349 (1979).

[28] J. K. Deng, W. C. Ma, J. H. Hamilton, A. V. Ramayya, J. Rikovska, N. J. Stone, W. L. Croft, R. B. Piercey, J. C. Morgan, and P. F. Mantica, Jr., Nucl. Instrum. Methods Phys. Res. A **317**, 242 (1992).

[29] H. J. Rose and D. M. Brink, Rev. Mod. Phys. **39**, 306 (1967).

[30] G. Gürdal and E. A. McCutchan, Nucl. Data Sheets **136**, 1 (2016).

[31] W. Nazarewicz, J. Dudek, R. Bengtsson, T. Bengtsson, and I. Ragnarsson, Nucl. Phys. A **435**, 397 (1985).

[32] `http://www.volya.net/index.php?id=cosmo`.

[33] M. Honma, T. Otsuka, T. Mizusaki, and M. Hjorth-Jensen, Phys. Rev. C **80**, 064323 (2009).

[34] B. A. Brown and W. A. Richter, Phys. Rev. C **74**, 034315 (2006).

[35] Khalifeh Abusaleem and Balraj Singh, Nucl. Data Sheets **112**, 133 (2011).

[36] Alan L. Nichols, Balraj Singh, and Jagdish K. Tuli, Nucl. Data Sheets **113**, 973 (2012).

[37] Balraj Singh and Jun Chen, Nucl. Data Sheets **178**, 41 (2021).

[38] A. Filevich, A. Ceballos, M. A. J. Mariscotti, P. Thieberger, and E. Der Mateosian, Nucl.

Phys. A **295**, 513 (1978).

[39] J. Döring, S. L. Tabor, J. W. Holcomb, T. D. Johnson, M. A. Riley, and P. C. Womble, Phys. Rev. C **49**, 2419 (1994).

[40] J. Döring, D. Pantelică, A. Petrovici, B. R. S. Babu, J. H. Hamilton, J. Kormicki, Q. H. Lu, A. V. Ramayya, O. J. Tekyi-Mensah, and S. L. Tabor, Phys. Rev. C **57**, 97 (1998).

[41] A. J. Kreiner and M. A. J. Mariscotti, Phys. Rev. Lett. **43**, 1150 (1979).

[42] R. Wyss, F. Lidén, J. Nyberg, A. Johnson, D. J. G. Love, A. H. Nelson, D. W. Banes, J. Simpson, A. Kirwan, and R. Bengtsson, Nucl. Phys. A **503**, 244 (1989).

TABLE I: Parent-state excitation energies (E_x), transition energies (E_γ), spin-parity assignments for the initial (J_i^π) and final (J_f^π) state, relative intensities (I_γ), DCO ratios ($R_{\rm DCO}$), experimental ($P_{\rm exp}$) and theoretical ($P_{\rm thy}$) linear polarizations, and multipolarities (σL) associated with the γ rays observed from the high-spin decay of ^{70}Ga.

E_x (keV)	E_γ (keV)	J_i^π	J_f^π	I_γ[1]	$R_{\rm DCO}$	$P_{\rm exp}$	$P_{\rm thy}$[2]	σL
690.8(1)	690.8(1)	2^-	1^+	100(3)[3]	0.53(4)	0.18(7)	0.12[4]	$E1$
878.5(1)	187.7(1)	4^-	2^-	89(2)	1.16(12)	0.4(2)	0.43(10)	$E2$
1033.5(1)	155.0(1)	5^-	4^-	74(2)	0.57(4)	−0.4(2)	−0.4(3)	$M1/E2$
1101.5(1)	67.9(2)	4^-	5^-	2(1)				$M1/E2$
	410.7(1)	4^-	2^-	2.4(3)	1.5(6)[5]			$E2$
1179.8(2)	146.5(1)	5^-	5^-	3.0(5)	1.4(4)			$M1/E2$
	301.2(1)	5^-	4^-	8.2(4)	0.65(18)	−0.9(6)	−0.4(3)	$M1/E2$
1233.3(1)	199.8(1)	6^-	5^-	65(2)	0.57(4)	−0.7(2)	−0.4(3)	$M1/E2$
	354.4(3)	6^-	4^-	2.9(3)				$E2$
1370.3(1)	137.1(1)	7^-	6^-	42(2)	0.54(4)	−0.7(5)	−0.4(3)	$M1/E2$
	190.8(3)	7^-	5^-	3.3(7)	0.9(3)			$E2$
	336.6(1)	7^-	5^-	2.9(4)	0.9(3)			$E2$
1537.5(1)	167.0(2)	6^-	7^-	2.1(2)	0.6(2)			$M1/E2$
	304.2(1)	6^-	6^-	4.5(3)	0.8(3)			$M1/E2$

	435.9(2)	6^-	4^-	2.1(5)				$E2$
1686.2(2)	315.9(3)	6^-	7^-	2(1)	0.85(18)[6]			$M1/E2$
	652.7(2)	6^-	5^-	1.9(4)	0.5(2)			$M1/E2$
2030.1(2)	796.8(2)	(6^-)	6^-	2.5(7)	0.8(4)			$(M1/E2)$
	996.4(4)	(6^-)	5^-	1.3(5)				$(M1/E2)$
2283.7(3)	913.1(5)	6^+	7^-	2.7(5)				$E1$
	1104.1(3)	6^+	5^-	3.9(5)	0.5(2)			$E1$
2306.7(1)	769.4(2)	7^+	6^-	2.1(3)				$E1$
	936.4(1)	7^+	7^-	7.1(6)	1.1(2)	−0.7(8)	−0.72[4]	$E1$
2600.2(1)	293.0(4)	8^+	7^+	0.6(2)				$M1/E2$
	315.9(3)	8^+	6^+	5.3(3)	0.85(18)[6]			$E2$
	1229.9(1)	8^+	7^-	15.5(6)	0.48(13)	0.3(3)	0.33[4]	$E1$
2650.4(1)	1280.1(1)	9^-	7^-	12.0(6)	0.80(17)	0.3(5)	0.65[4]	$E2$
2884.7(1)	284.5(1)	9^+	8^+	8.4(4)	0.51(7)	−0.5(3)	−0.34[4]	$M1/E2$
3515.9(2)	915.7(2)	10^+	8^+	11(2)	0.9(2)	0.6(6)	0.61[4]	$E2$
3875.4(3)	359.5(5)	(11^+)	10^+	4(3)				$(M1/E2)$
	990.7(1)	(11^+)	9^+	3.6(6)	0.9(4)			$(E2)$
4166.6(4)	1516.2(2)	(11^-)	9^-	2.2(3)	1.1(6)			$(E2)$
4428.5(4)	553.1(2)	(11^+)	(11^+)	1.9(3)	1.0(4)			$(M1/E2)$

[1] Determined at 90° and corrected for angular distribution effects (see text).
[2] Calculated using measured a_2, a_4, and δ values from Ref. [8] (unless otherwise noted) with a sign that assumes the given multipolarity.
[3] Intensities normalized to this transition.
[4] Determined from theoretical angular distribution coefficients based on the given J_i and J_f values and assuming a stretched ($\delta = 0$) transition.
[5] Determined from a gate on the 691-keV $E1$ transition.
[6] DCO ratio of the doublet.